N87-11211

CONSTITUTIVE MODELING FOR ISOTROPIC MATERIALS

Ulric S. Lindholm
Southwest Research Institute

INTRODUCTION

This report presents results of the first year of effort on a program with the objective to develop a unified constitutive model for finite-element structural analysis of turbine engine hot section components. The program is a joint effort between Southwest Research Institute and Pratt & Whitney Aircraft.

The initial two year program includes a state-of-the-art review of applicable constitutive models with selection of two for detailed comparison with a wide range of experimental test. The experimental matrix contains uniaxial and biaxial tensile, creep, stress relaxation and cyclic fatigue tests at temperatures to 1093°C and strain rates from 10^{-7} to 10^{-3} sec^{-1}. Some non-isothermal TMF cycles will be run also. The constitutive models will be incorporated into the MARC finite element structural analysis program with a demonstration computation made for an advanced turbine blade configuration. In the code development work, particular emphasis is being placed on developing efficient integration algorithms for the highly non-linear and stiff constitutive equations. Another area of emphasis is the appropriate and efficient methodolgy for determining constitutive constants from a minimum extent of experimental data.

CONSTITUTIVE MODELS

An extensive review of currently available unified constitutive models was made from which a review is given in references 1 and 2. In a "unified" theory, the inelastic strain rate term, $\dot{\varepsilon}^p$, is considered to include all strains that are not elastic; i.e., the difference between the total strain and the elastic strain, $\underset{\sim}{\varepsilon} - \underset{\sim}{\varepsilon}^e$. Thus, unified implies that all aspects of inelastic behavior such as plastic flow, creep and stress relaxation are included in the single function, $\dot{\underset{\sim}{\varepsilon}}^p$, and are simply representative response characteristics for different loading histories. In such theories, inelastic behavior may be described with or without the use of a yield function or concept of plastic potential. Those chosen here for further study do not employ a yield criteria and are based on internal variables to describe "yielding" and strain or work hardening behavior.

Two particular constitutive models were chosen for detailed study and comparison with experimental data. These were developed by Bodner and Partom (B-P) (ref. 3) and by Walker (WK) (ref. 4). Both models had considerable prior application to high-temperature alloys used in gas turbine components. Most unified models are of the basic form

$$\frac{\underset{\sim}{\sigma} - \underset{\sim}{X}_1}{X_2} = f(\dot{\underset{\sim}{\varepsilon}}^p, T) \qquad (1)$$

PRECEDING PAGE BLANK NOT FILMED

here σ, $\dot{\varepsilon}^p$ and T are stress, inelastic strain rate and temperature, respectively. Generally, two independent internal variables are used, $\underset{\sim}{X}_1$ a tensor quantity describing directional material hardening (often referred to as a back stress, equilibrium stress, or kinematic hardening variable) and X_2 a scalar measure of the magnitude of isotropic hardening. The evolutionary equations for both internal variables are usually of the hardening-recovery form,

$$\dot{X}_i = h(X_i)\ \dot{M} + r(X_i,T) \qquad (2)$$

where M is a physical measure of hardening and h and r are hardening and recovery functions.

The WK model uses a power law for the kinetic term, $f(\dot{\underset{\sim}{\varepsilon}}^p,T)$, and plastic strain as the measure of hardening M. The B-P model uses an exponential form in the kinetic term and plastic work for M. The other major difference between the two models is that B-P avoids the use of the back stress $\underset{\sim}{X}_1$ and encorporates both isotropic and directional hardening in a partitioning of $\underset{\sim}{X}_2$. For a more detailed comparison see references 1 and 2.

EXPERIMENTAL PROGRAM

An extensive test program is underway to generate a comprehensive set of data which is to be compared with model predictions. A cast nickel base alloy, B1900+Hf, with grain size of ASTM No. 1 to 2 is used for the specimens shown in figure 1. As indicated, tensile, creep, isothermal cyclic, thermomechanical cyclic and biaxial (tension-torsion) tests are being performed. To date the tensile, creep and isothermal cyclic tests are complete. Sample results, including correlations with the B-P model, are given in figures 2-5 (correlations with the WK model are being generated also but were not available as of this writing). All model correlations are made with a single set of material constants.

Figure 2 shows the correlation for tensile curve at three temperatures. In the process of determining the constants associated with work hardening in the B-P model, the experimental hardening data was plotted as in figure 3 where $\gamma = d\sigma/dW_p = d\sigma/\sigma\ d\varepsilon^p$. Analysis shows that the data at each strain rate can be closely approximated as the sum of two linear curves, whose slopes and intercepts yield the coefficients for the isotropic and kinematic hardening terms. Thus, it appears possible to predict cyclic behavior from monotonic stress-strain curves. This conclusion needs further verification but holds potential for reducing the testing required for constitutive constant determinations. Another observation from figure 3 is that a change in strain rate does not change the hardening rate (slope) in agreement with the separation of kinetic and hardening terms in equation (1). The slopes do change with temperature because of thermal recovery of hardening (eq. (2)).

Figure 4 shows the small strain ($0.2\%\varepsilon^p$) flow stress over the range of temperature and strain rate studied. Inflections in the curves at the intermediate temperatures result from the influence of thermal recovery at lower rates and higher temperatures. At low temperatures and high rates, thermal recovery is not significant.

An example of initial and saturated cyclic loops at 538°C is given in figure 5. Agreement between experiment and theory is reasonable in this and other cases examined considering the same constants are used for figures 2, 4 and 5. More complex loops with creep or relaxation holds during a cycle will be correlated during the second year along with cyclic biaxial data.

IMPLEMENTATION IN F.E. CODE

Both models are being implemented for use with the MARC finite element code. The code will subsequently be used to analyze a notched tensile round test specimen used as a benchmark experiment and also an advanced turbine blade configuration. The latter will be a numerical demonstration only. Several numerical methods are being studied for implementing the models in the MARC code. Integration methods for viscoplastic theories to be examined include:

(1) Explicit Euler integration with both a fixed and self-adaptive time step
(2) The implicit noniterative, selfcorrecting solution (NONSS) method of Miller and Tanaka (ref. 5)
(3) Implicit integration of the integral form of the equations.

It is expected that each theory will be coded with at least two numerical intergration algorithms.

SUMMARY

The work to date is encouraging with respect to the ability of unified constitutive theories to predict with reasonable accuracy quite complex time and temperature dependent inelastic material behavior. Also encouraging, at this point, is the possibility of determining all necessary constitutive constants from perhaps as little as monotonic tensile curves at several temperatures and strain rates. Such data is generally available for alloys of interest. For implementation of the models in finite element codes and efficient structural analysis, optimum numerical integration schemes need further development.

REFERENCES

1. Chan, K. S.; Bodner, S. R.; Walker, K. P.; and Lindholm, U. S.: A Survey of Unified Constitutive Theories. Second Symposium on Nonlinear Constitutive Relations for High Temperature Applications, Cleveland, Ohio, June 1984.

2. Lindholm, U. S.: Constitutive Modeling for Isotropic Materials. First Annual Report, NASACR-174718, May 1984.

3. Bodner, S. R. and Partom, Y.: ASME J. of Applied Mechanics, Vol. 42, 1975, p. 385.

4. Walker, K. P.: NASA Contract Report NASA CR 165533, 1981.

5. Tanaka, T. G.: Deformation of Metals and Alloys. Ph.D. Thesis, Stanford University, 1983.

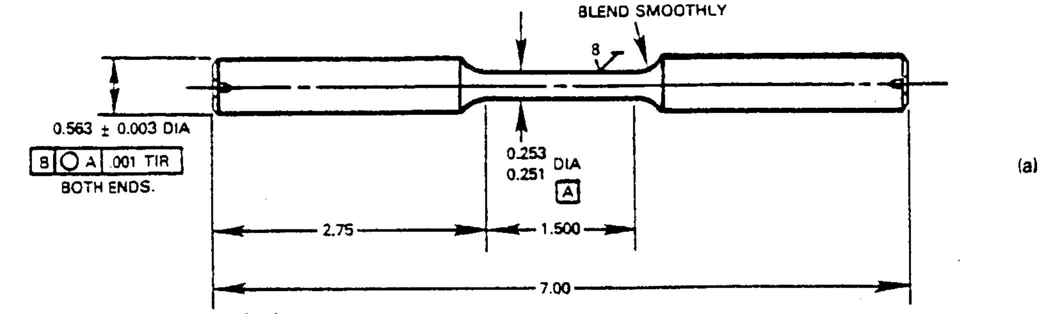

(a) Monotonic tensile/creep specimen

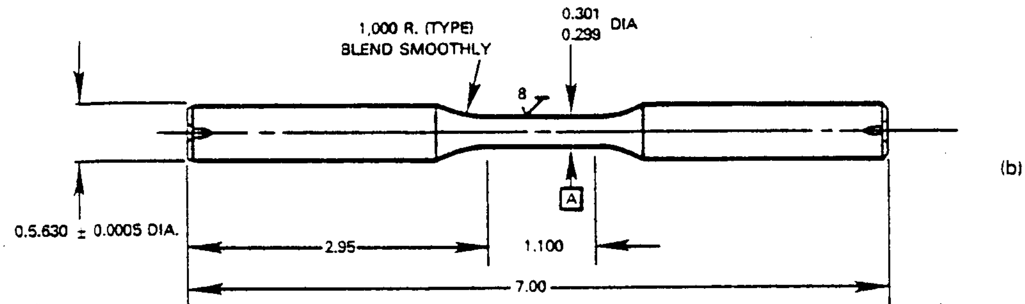

(b) Isothermal cyclic specimen

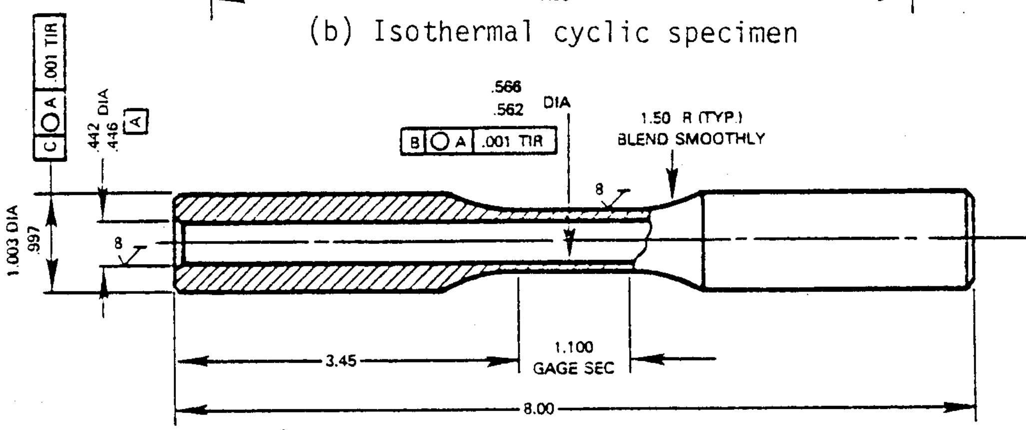

(c) Thermomechanical cyclic specimen

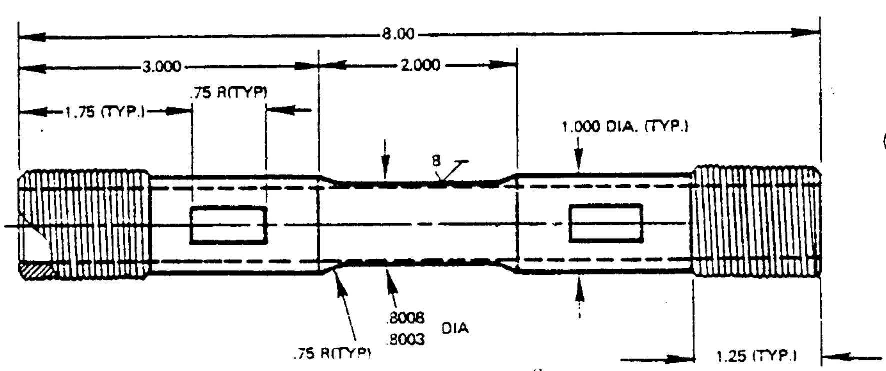

(d) Isothermal biaxial test specimen

Figure 1. Specimen Designs Utilized in Various Constitutive Tests.

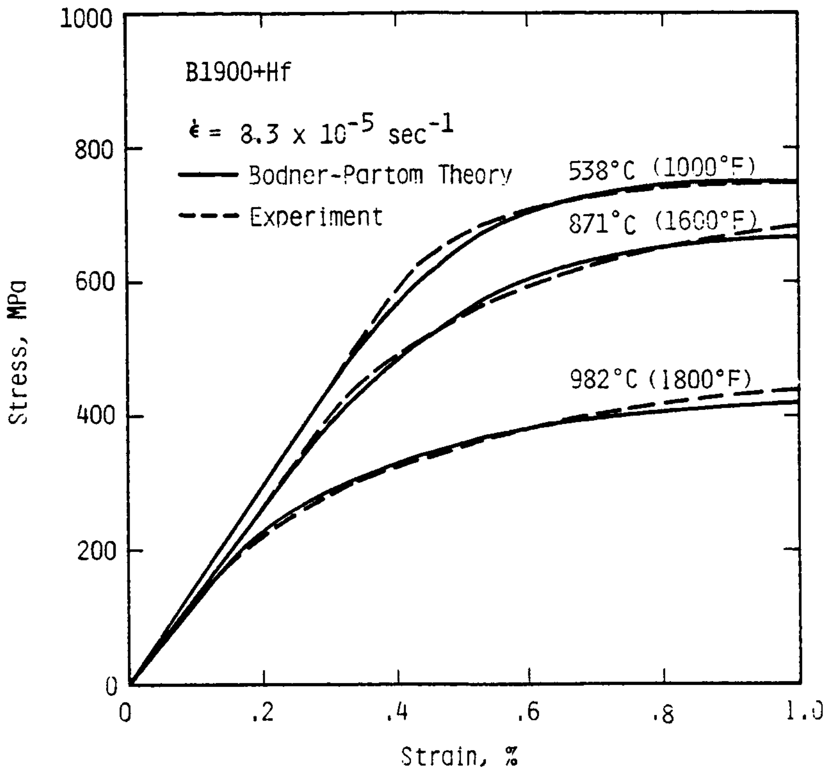

Figure 2. A Comparison of the Calculated (Bodner-Partom Theory) and the Experimental Stress-Strain Curves of B1900+Hf at 538, 871 and 982°C.

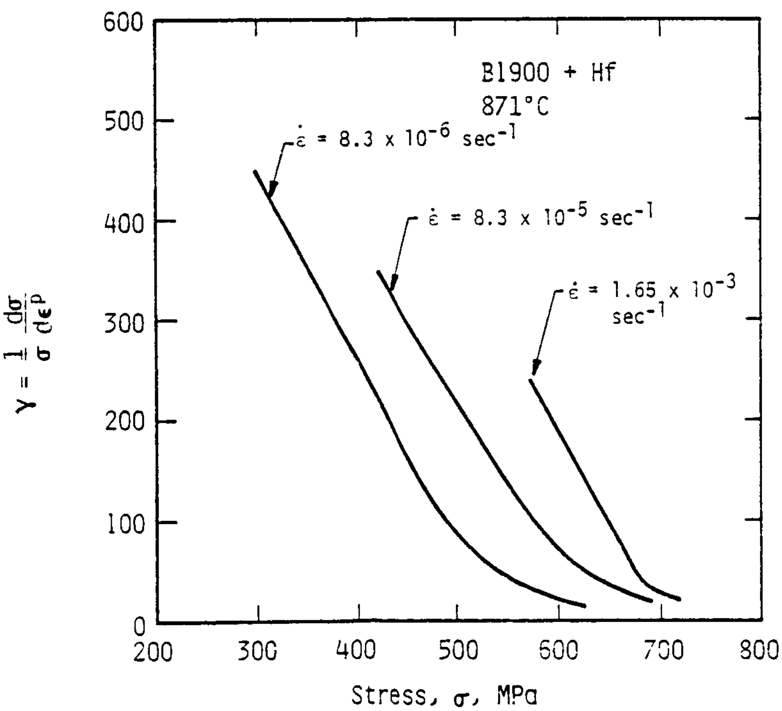

Figure 3. Work Hardening Behavior of B1900+Hf at Three Strain Rates and 871°C.

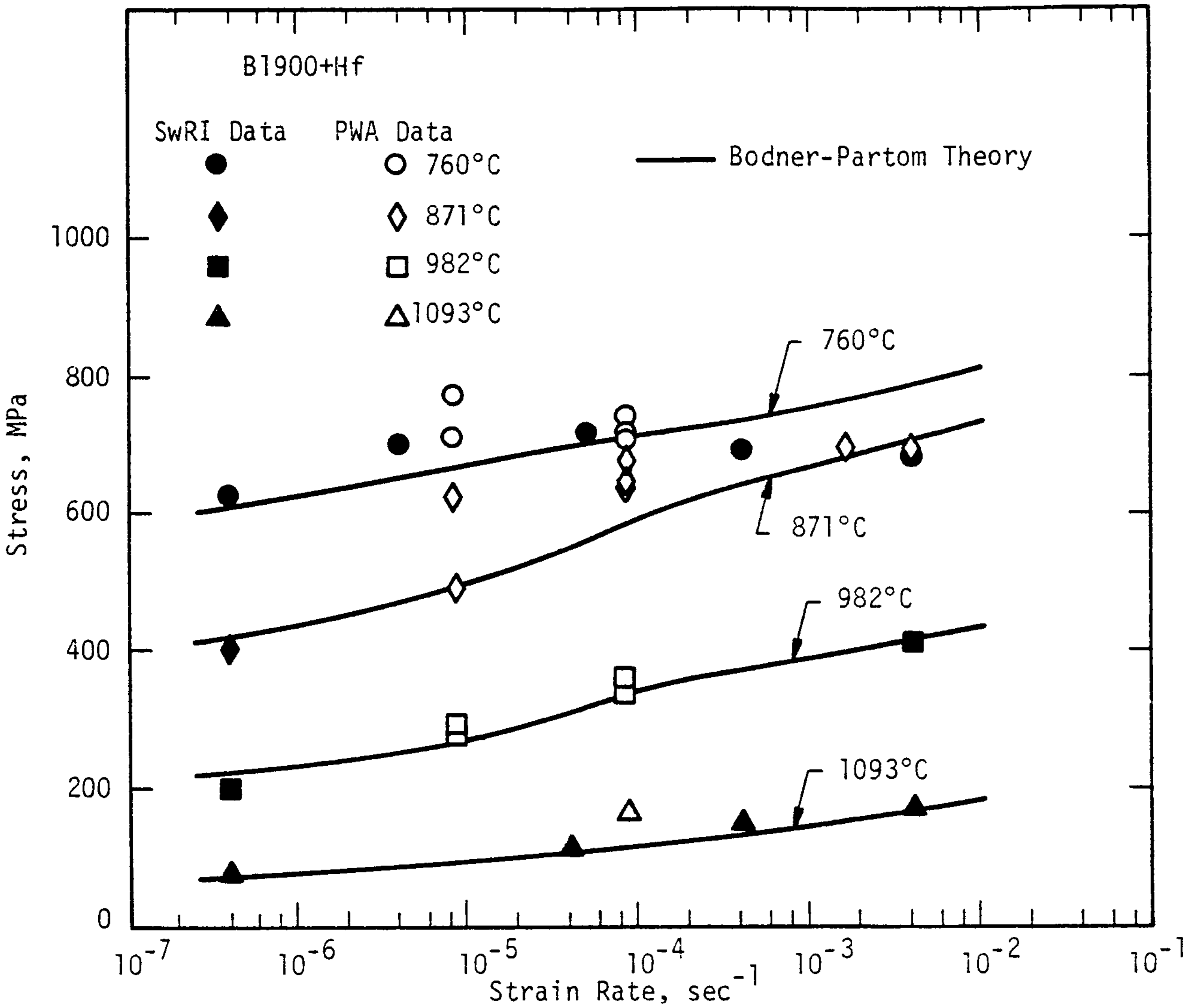

Figure 4. Temperature and Strain-Rate Dependence of 0.2% Offset Yield Stress for B1900+Hf.

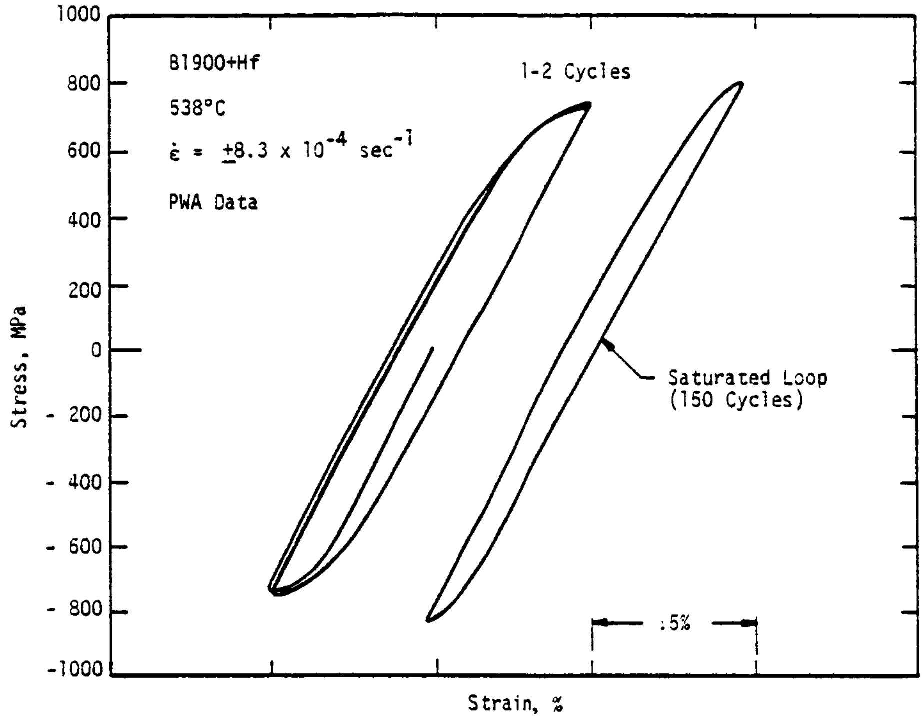

(a) Experiment

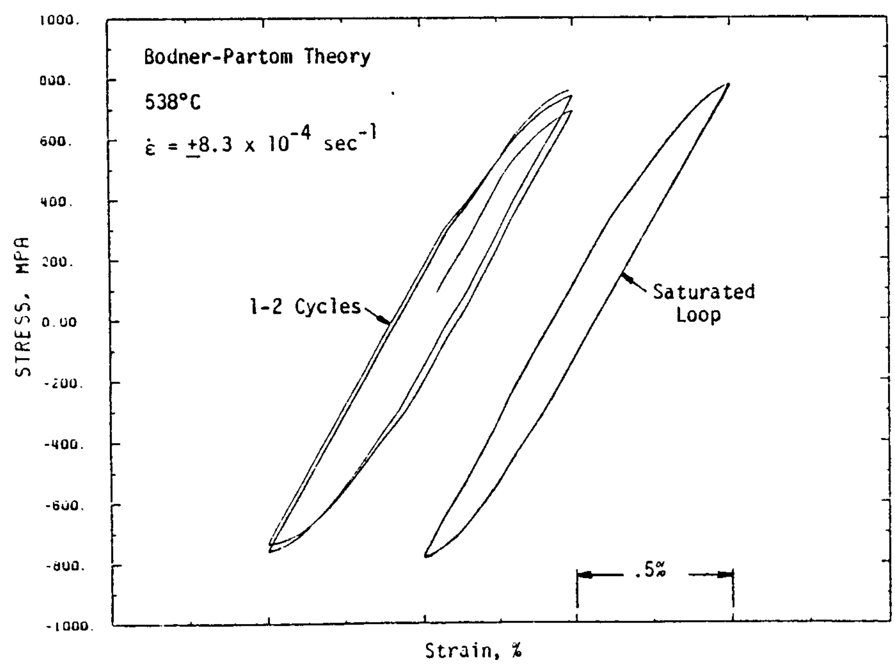

(b) Bodner-Partom Theory

Figure 5. A Comparison of the Calculated (Bodner-Partom Theory) and the Experimental Hysteresis Loops After 1-2 Cycles and at Cyclic Saturation.